PRIFYSGOL
ABERYSTWYTH
UNIVERSITY

Aberystwyth University

Neoclerodane Diterpenoids from Reehal Fatima, Teucrium yemense

Nur-e-Alam, Mohammad ; Yousaf, Muhammad; Ahmed, Sarfaraz; Al-Sheddi, Ebtesam S.; Shah, Ifat;
Fazakerley, David; Bari, Ahmed; Ghabbour, Hazem A.; Threadgill, Michael D.; Whatley, Kezia; Hoffmann, Karl;
Al-Rehaily, Adnan J.

Neoclerodane Diterpenoids from Reehal Fatima, *Teucrium yemense*

Mohammad Nur-e-Alam,*[†] Muhammad Yousaf,[†] Sarfaraz Ahmed,[†] Ebtesam S. Al-Sheddi,[†] Ifat Parveen,[‡] David M. Fazakerley,[‡] Ahmed Bari,[§] Hazem A. Ghabbour,[§] Michael D. Threadgill,[⊥] Kezia C. L. Whatley,[‡] Karl F. Hoffmann,[‡] and Adnan J. Al-Rehaily*[†]

[†]Department of Pharmacognosy and [§]Department of Pharmaceutical Chemistry, College of Pharmacy, King Saud University, P.O. Box. 2457, Riyadh 11451, Kingdom of Saudi Arabia.

[‡]Institute of Biological, Environmental & Rural Sciences (IBERS), Aberystwyth University, Aberystwyth SY23 3DA, United Kingdom.

[⊥]Drug & Target Discovery, Department of Pharmacy and Pharmacology, University of Bath, Claverton Down, Bath, BA2 7AY, United Kingdom.

ABSTRACT: *Teucrium yemense* (Defl) (*T. yemense*), locally known as Reehal Fatima, is a medicinal plant commonly grown in Saudi Arabia and Yemen. Phytochemical investigation of the aerial parts of *T. yemense* yielded six new neoclerodane diterpenoids, namely fatimanol A-E (**1**, **2**, **3**, **5**, **6**) and fatimanone (**4**), and the known teulepicephin (**7**). As both the *Teucrium* genus and the related *Lamiaceae* family have previously been widely reported to possess anthelmintic and antimicrobial activities, the structural and biological characterisation of the seven diterpenoids was pursued. The structures of the new compounds were elucidated from their 2D NMR and MS profiles, and by comparison to related compounds. The structure of fatimanol D (**5**) was confirmed by X-ray crystallographic analysis. The new structures contribute to the breadth of knowledge of secondary metabolites in this genus.

Teucrium is a polymorphic and cosmopolitan genus of herbaceous perennial plants belonging to the *Lamiaceae* family.[1] There are more than 340 species, including herbs, shrubs, and subshrubs, mainly distributed in South-East Asia, Central and South America, Mediterranean countries, and in the Middle East.[2] Saudi Arabia is one of the original centers of *Teucrium*, where there currently exist at least six species.[3] Interestingly, the genus *Teucrium* can be distinguished from other members of the *Lamiaceae* family, as the flowers lack the upper lip of the corolla.[4] *Teucrium* species have been used for more than 2000 years as diuretic, diaphoteric, antiseptic, and antipyretic agents.[4] Some species have also been reported to possess anti-feedant activities.[5,6] In Saudi Arabia, *Teucrium* species have been traditionally used to treat diabetes, whereas, in other locales, reported activities include insecticidal, anthelmintic, analgesic, anti-inflammatory, antioxidant, antiulcer, antispasmodic, antibacterial, and antifungal properties.[4,7−9] The diversity, richness, and variation of the species and the ability of the plant to produce a diverse array of biologically active secondary metabolites have led to much interest in this genus.[9] Previous phytochemical studies revealed that the plant is a rich source of essential oils, diterpenoids, flavonoids, and iridoids.[10,11] However, other compounds isolated include alkaloids, sterols, tannins, saponins, coumarins, and glycosides.[4,9]

In particular, *Teucrium yemense* (Defl.), locally known as Reehal Fatima, is a medicinal plant commonly grown in Saudi Arabia and in Yemen. In these regions, the plant has long been used to treat kidney diseases, rheumatism and diabetes.[9,12,13] *T. yemense* is an aromatic plant possessing sessile oblanceolate leaves and dense terminal heads of pink to scarlet to purple flowers.[3] In particular, the neoclerodanes are of interest as they have been reported to encompass wide-ranging biological and pharmacological properties.[7,9,14−17] While *Teucrium* species are

largely known for their essential oils, a number of novel neoclerodane diterpenoids have been isolated.[10,14,18,19]

To date, the medicinal active components of *T. yemense* are still unknown. In the present study, the isolation, purification, and structural elucidation of six new neoclerodanes from *T. yemense* are reported. The compounds were tested against a range of gram-positive (*Staphylococcus aureus* and *Bacillus cereus*) and gram-negative (*Escherichia coli* and *Pseudomonas aeruginosa*) microorganisms and mammalian cytotoxicity studies were carried out against a human liver-derived cell line (HepG2 cell line). Furthermore, compounds **1-7** were assessed for anthelmintic activities against the larval schistosomula lifecycle stage of *Schistosoma mansoni,* a parasitic trematode responsible for transmitting schistosomiasis in Saudi Arabia and Yemen.[20]

RESULTS AND DISCUSSION

The dried aerial parts of the plant were defatted and extracted with MeOH. This solvent was evaporated and the residue was extracted with EtOAc. This extract was separated by column chromatography on silica gel. Repeated column chromatography and HPLC yielded seven pure compounds (Chart 1). Their structures were elucidated *via* 1D and 2D NMR and HRESIMS data. The absolute configurations cannot be confirmed from these data but are assumed based on literature precedent for related compounds.[10,21,22]

Compound 1. The HRESIMS of **1** showed a peak at *m/z* 483.2222 corresponding to [M + H]$^+$ for $C_{24}H_{34}O_{10}$ (calcd. 483.2221) (Figure S1, Supporting Information). A peak was also observed at *m/z* 505.2040 (calcd. 505.2050), corresponding to [M + Na]$^+$ for this molecular formula. The NMR spectra showed the appropriate numbers of ^{1}H and ^{13}C signals (Figures S2,

S3, Supporting Information). Fragment ions were observed with *m/z* 465 (loss of H_2O, suggesting the presence of a hydroxy function) and *m/z* 423 (loss of HOAc, suggesting the presence of an acetoxy group). The core structure was shown to be a decalin, by a combination of NMR techniques (Table 1) (Figures S2-S7, Supporting Information), and related to the neoclerodane series of diterpenoids.[10,21,22]

The ^{1}H NMR spectrum showed a peak at δ_H 2.09 (6 H), correlating by HSQC to ^{13}C signals at δ_C 21.0 and 21.1 (Figures S2, S5, Supporting Information). Two ester carbonyl signals were observed at δ_C 172.6 and 172.7, showing the presence of two acetate moieties (Figure S3, Supporting Information). HMBC data linked these to ^{1}H signals at δ_H 4.65 (d, *J* = 12.0 Hz) and 4.44 (d, *J* = 12.0 Hz) as well as to ^{1}H signals at δ_H 4.04 (d, *J* = 12.0 Hz) and 3.98 (d, *J* = 12.0 Hz), indicating CH_2OAc units in asymmetric environments. Further HMBC correlation between the protons at δ_H 4.65 and 4.44 to ^{13}C signals at δ_C 74.3 (C-6), 70.5 (C-4), and 47.3 (C-10) confirmed the location of one acetoxymethyl unit at C-5 (Figure S6, Supporting Information). HMBC cross-peaks between the protons at δ_H 4.04 and 3.98 to ^{13}C signals at δ_C 30.8 (C-11), 35.2 (C-8), 47.3 (C-10), and δ_C 42.8 (C-9) confirmed that the other acetoxymethyl unit was attached to C-9.

The C-4 *spiro*-oxirane functionality was shown by the presence of a CH_2 group [δ_H 3.22 (d, *J* = 4.0 Hz) and 3.01 (d, *J* = 4.0 Hz), δ_C 44.3], with the small geminal coupling constant and shielded chemical shifts reflecting the strained three-membered ring. Relatively weak HMBC cross-peaks were seen between the proton at δ_H 3.01 and C-3 (δ_C 66.4) and C-5 (46.4), along with two-bond correlations between the carbon at δ_C 70.5 and the methylene oxirane proton signals, confirming the C-4 *spiro*-oxirane moiety. The substituted 5-hydroxy-3-ethylfuran-2(5*H*)-

Chart 1. Structures of new neoclerodanes **1-6** and known analogue **7**, isolated from *T. yemense*.
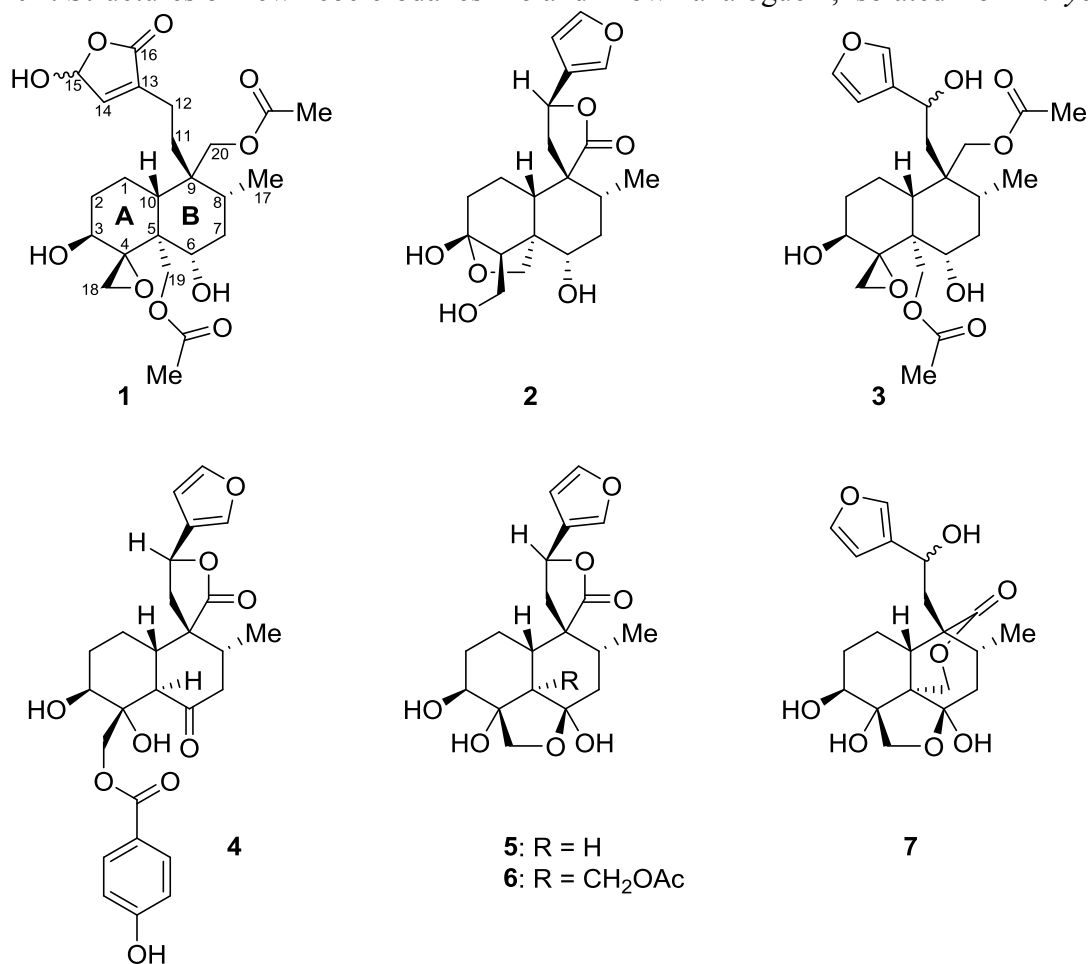
one side-chain was identified *via* a carbonyl at δ_C 173.9 (C-16) and a hemiacetal carbon at δ_C 99.0 (HMBC to the proton at δ_H 6.06), along with CH$_2$ signals at δ_C 30.8 (δ_H 1.71) and 19.3 (δ_H 2.11, 2.21) and appropriate HMBC correlations. HMBC correlation between H$_2$-20 (δ_H 4.04 and 3.98) and C-11 confirmed the location of this side-chain.

The relative configurations were also established *via* NMR data (Figures S2-S7, Supporting Information). NOESY cross-peaks were observed from H-10 (δ_H 1.66) to H-8 (δ_H 1.83) and to H-6 (δ_H 3.79), confirming that all three hydrogens were cofacial and axial. The NOESY correlation between one of the diastereotopic CH$_2$OAc protons (δ_H 4.65) and H-3 (δ_H 4.01) also located these on the same face of the central bicycle and showed that both were also

axial. Thus the CH$_2$OAc group at C-5 and H-10 are *trans*-diaxially disposed and the bicycle is confirmed as a *trans*-decalin. The relative configuration at the quaternary C-9 was also established by NOESY. Since H-8 is axial and on the β-face, then CH$_3$-17 must be equatorial and on the α-face. A strong NOESY interaction between CH$_3$-17 (δ_H 0.98) and the other CH$_2$OAc (δ_H 3.98, 4.04), showed that this CH$_2$OAc was axial on the α-face and, therefore, that the substituted 5-hydroxy-3-ethylfuran-2(5*H*)-one unit was equatorial on the β-face. Finally, the CH$_2$ of the *spiro*-oxirane was placed on the β-face by a NOESY correlation between the oxirane CH (δ_H 3.22) and H-6 (δ_H 3.79). The configuration at C-15 could not be determined. Thus we propose structure **1** for fatimanol A.

Compound 2. The HRESIMS of **2** showed a peak at *m/z* 401.1567, corresponding to [M + Na]$^+$ for a molecular formula of C$_{20}$H$_{26}$O$_7$ (calcd. [M + Na] 401.1576) (Figure S8, Supporting Information). A peak at *m/z* 379.1747, corresponding to [M + H]$^+$ (calcd. 379.1757), confirmed the molecular formula. The NMR spectra showed the appropriate numbers of ^{1}H and ^{13}C signals (Figures S9, S10, Supporting Information). No MS peaks corresponding to loss of 60 Da were observed, suggesting the absence of acetoxy groups, but the sequence, *m/z* 379 → *m/z* 361 → *m/z* 343 indicated the presence of at least two hydroxy groups.

The NMR data (Table 1), including COSY, NOESY, HSQC, and HMBC spectra (Figures S9-S14, Supporting Information), indicated a neoclerodane skeleton, as for **1**. However, the details of the structure, conformation, and configuration differ from those of **1**.
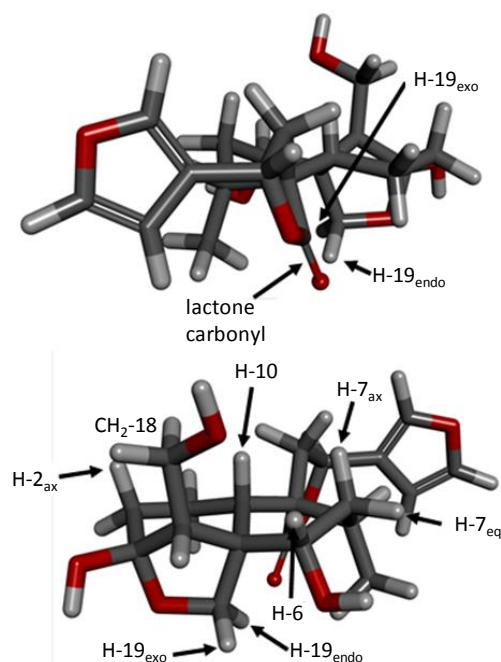

Figure 1. Views of MM2-minimised structure of **2**, showing the positioning of the 19$_{endo}$-H in the deshielding plane of the lactone carbonyl and the chair-boat conformation of the *trans*-decalin.

Firstly, the hemiacetal group at C-3 was shown by the chemical shift δ_C 106.2. This may, in principle, be formed by cyclization of the corresponding carbonyl with a hydroxy group at C-18, at C-6, or at C-19. The first possibility can be dismissed, in that an oxetane moiety would be too strained to exist as part of a hemiacetal. Formation of a five-membered cyclic hemiacetal unit with the oxygen attached to C-19 was confirmed by a HMBC cross-peak between the H-19 signal at δ_H 4.76 and the C-3 signal at δ_C 106.2. Thus the -CH_2O- bridge spanning C-3 and C-6 is confirmed.

The C-9 *spiro*-tetrahydrofuranone unit was established through the chemical shift of H-12 (δ_H 5.51), which corresponds to furanCH(R)O(C=O). The NOESY spectrum in the region δ_H 2.0–2.7 is unclear, precluding definite assignment of the configuration at C-9, so it is assigned by analogy with **1**. It is notable that the diastereotopic CH_2-19 protons resonate at very different frequencies (δ_H 4.76 and 3.41); there must be a transannular effect which moves the signal at δ_H 4.76 so far downfield from the chemical shift predicted by σ-bond inductive effects alone. Examination of an MM2-minimized structure of **2** (Figure 1) provides the explanation. The 19_{endo} hydrogen is held rigidly in the optimal shielding plane of the magnetically anisotropic lactone carbonyl. Not only does this differentiate H-19_{endo} (δ_H 4.76) and H-19_{exo} (δ_H 3.41) but it also confirms that the lactone carbonyl is on the α-face and that the absolute configuration at C-9 is *R*.

H-10 resonates at δ_H 2.36 (dd, J = 5.0 and J = 12.5 Hz); these couplings correspond to $^3J_{ax-ax}$ and $^3J_{ax-eq}$, respectively, with CH_2-1. Thus H-10 must be axial. CH_2-19 must also be axial to be able to form the bridge; thus the bicycle is a *trans*-decalin. Ring A has a chair conformation, confirmed by axial-axial NOESY connections from one of the CH_2-18 hydrogens

at δ_H 3.85 to H-10 (δ_H 2.36) and H-2$_{ax}$ (δ_H 1.49). MM2-minimization (Figure 1) of the structure

of **2** suggests that ring B may be a distorted boat, with the "prow" and "stern" at C-7 and C-10,

respectively. This is supported by the signal for H-6 having no coupling with $J > 5$ Hz, *i.e.* no

trans-diaxial coupling. H-15 and H-16 of the aromatic furanyl moiety resonate at δ_H 7.54 and

7.60, respectively, and the shielded H-14 at δ_H 6.50. The furanyl unit is attached to the lactone

moiety at C-12, as confirmed by HMBC cross-peaks between H-12 (δ_H 5.51) and C-14 (δ_C

109.3) and C-16 (δ_C 141.5). Thus structure **2** is proposed for fatimanol B.

Compound 3. The HRESIMS of **3** shows major ions at *m/z* 467.2272 [M + H]$^+$ for a

molecular formula $C_{24}H_{34}O_9$ (calcd. 467.2281) and at *m/z* 489.2089 [M + Na]$^+$ (calcd. 489.2101),

confirming the molecular formula (Figure S15, Supporting Information). The NMR spectra

showed the appropriate numbers of ^1H and ^{13}C signals (Table 1 and Figures S16, S17,

Supporting Information). The fragmentation *m/z* 467 $\rightarrow$ *m/z* 407 suggests the presence of an

acetoxy group and the fragmentation *m/z* 467 $\rightarrow$ *m/z* 449 suggests the presence of a hydroxy

group.

Table 1. ^1H and ^{13}C NMR Spectroscopic Data for **1-3** in Methanol-d_4 [δ_H, Multiplicity, (J (Hz))] [δ_C, Type]

	1		2		3	
position	δ_H	δ_C	δ_H	δ_C	δ_H	δ_C
1	1.94 m	21.9, CH_2	2.10 m	23.9, CH_2	1.79 dd, (15.0, 2.5)	22.3, CH_2
	1.92 m		1.58 m		2.13 m	
2	2.16 m	34.5, CH_2	1.65 m	33.6, CH_2	2.11 m	34.4, CH_2
	1.36 m		1.49 m		1.39 m	
3	4.01 m	66.4, CH	-	106.2, C_q	4.02 (dd, 11.5, 4.5)	66.6, CH
4	-	70.5, C_q	2.02 d (10.0)	58.5, CH	-	70.6, C_q

9

5	-	46.4, C$_q$	-	51.3, C$_q$	-	46.4, C$_q$
6	3.79 t (8.0)	74.3, CH	3.72 br s	72.2, CH	3.78 dd (11.5, 5.0)	74.5, CH
7	1.63 m	35.1, CH$_2$	1.87 t (14) 1.60 m	35.1, CH$_2$	1.66 m 1.58 m	35.5, CH$_2$
8	1.83 m	35.2, CH	2.20 m	32.7, CH	1.87 m	35.2, CH
9	-	42.8, C$_q$	-	53.8, C$_q$	-	43.2, C$_q$
10	1.66 m	47.3, CH	2.36 dd (12.5, 5.0)	39.6, CH	2.21 dd (12.0, 2.0)	47.4, CH
11	1.71 m	30.8, CH$_2$	2.62 dd (14.0, 8.5) 2.49 dd (14.0, 9.0)	45.3, CH$_2$	1.91 dd (15.5, 8.5) 1.80 dd (15.5, 3.5)	40.3, CH$_2$
12	2.21 m 2.11 m	19.3, CH$_2$	5.51 t (8.5)	73.9, CH	4.77 dd (8.5, 2.5)	63.3, CH
13	-	137.9, C$_q$	-	126.7, C$_q$	-	132.4, C$_q$
14	7.02 s	146.7, CH	6.50 s	109.3, CH	6.42 s	109.6, CH
15	6.06 s	99.0, CH	7.54 s	145.5, CH	7.46 s	144.7, CH
16	-	173.9, C=O	7.60 s	141.5, CH	7.46 s	139.8, CH
17	0.98 d (7.0)	16.5, CH$_3$	0.97 d (6.5)	17.0, CH$_3$	0.91 d (7.0)	16.6, CH$_3$
18	3.22 d (4.0) 3.01 d (4.0)	44.3, CH$_2$	3.85 t (10.5) 3.60 dd (10.5, 1.5)	57.5, CH$_2$	3.18 d (3.5) 3.00 d (3.5)	44.0, CH$_2$
19	4.65 d (12.0) 4.44 d (12.0)	63.7, CH$_2$	4.76 d (8.5) 3.41 d (8.5)	71.6, CH$_2$	4.71 d (12.0) 4.43 d (12.0)	63.8, CH$_2$
20	4.04 d (12.0) 3.98 d (12.0)	66.9, CH$_2$	-	180.5, C=O	3.97 d (12.0) 3.90 d (12.0)	66.7, CH$_2$
1′	-	172.7, C=O			-	172.8, C=O
2′	2.09 s	21.1, CH$_3$			2.10 s	21.1, CH$_3$
3′	-	172.6, C=O			-	172.5, C=O
4′	2.09 s	21.0, CH$_3$			2.08 s	21.1, CH$_3$

The combined NMR spectroscopic data of **3** showed a structure similar to that of **1**, with structural differences in the furanyl unit and at C-12 (Figures S18-S21, Supporting Information). The chair-chair *trans*-decalin was confirmed as follows. H-10 (δ_H 2.21) is axial, as shown by couplings to H-1$_{ax}$ ($^3J_{ax\text{-}ax}$ = 12.0 Hz) and H-1$_{eq}$ ($^3J_{ax\text{-}eq}$ = 2.0 Hz). NOESY cross-peaks between the H-19 resonance at δ_H 4.71 and H-7$_{ax}$ (δ_H 1.66) place this CH$_2$OAc axial on the α-face, confirming a *trans*-ring junction. H-3 is also axial, as shown by the couplings to H-2$_{ax}$ ($^3J_{ax\text{-}ax}$ = 11.5 Hz) and H-2$_{eq}$ ($^3J_{ax\text{-}eq}$ = 4.5 Hz). Since H-10 and H-3 are both axial ring A must be in a chair conformation and the configuration at C-3 is confirmed. H-6 is axial as shown by its coupling to H-7$_{ax}$ ($^3J_{ax\text{-}ax}$ = 11.5 Hz) and H-7$_{eq}$ ($^3J_{ax\text{-}eq}$ = 5.0 Hz). H-6 also shows strong NOESY cross-peaks with H-10 and H-8, appropriate for cofacial axial protons.

As for **1**, the acetoxymethyl groups of **3** were located by HMBC experiments. H$_2$-19 (δ_H 4.43 and 4.71) showed cross-peaks with C-4 (δ_C 70.6), C-6 (δ_C 74.5), and C-10 (δ_C 47.4), in addition to the expected correlation with an ester carbonyl, showing that this CH$_2$OAc group was at C-5. H$_2$-20 (δ_H 3.90 and 3.97) correlated with C-8 (δ_C 35.2), C-10 (δ_C 47.4), C-11 (δ_C 40.3), and an ester carbonyl, linking this CH$_2$OAc unit to C-9. The heterocyclic part is shown to be a furanyl moiety in **3**, rather than the 5-hydroxyfuran-2(5*H*)-one unit of **1**, by the observation of aromatic proton signals at δ_H 6.42 (1 H) and 7.46 (2 H), along with ^{13}C signals at δ_C 109.6 (C-14), 132.4 (C-13), 139.8 (C-16), and δ_C 144.7 (C-15). The assignments were confirmed by HMBC and HSQC data. C-12 was shown to carry a hydroxy group, by the chemical shift of H-12 (δ_H 4.77), compared to H-12 (δ_H 5.51) in **2** where the oxygen function is part of a lactone moiety. The absolute configuration at C-12 could not be determined spectroscopically, although one may speculate that it may be *S*, by analogy with **2**. HMBC cross-peaks of H-12 with C-11,

C-13, C-14, and C-16 and of H$_2$-11 with C-13 and C-20 confirmed the structure of the 9β-substituent. Weak NOESY cross-peaks were seen between H$_3$-17 and both H$_2$-20 and H$_2$-11; this methyl group is equatorial, hence these correlations are not configurationally diagnostic for C-9. A strong NOESY correlation between H-10 and H-11, confirming the (9*R*) configuration with the -CH$_2$CH(OH)furanyl moiety occupying the β-face. Thus structure **3** is assigned to fatimanol C.

Compound 4. For **4**, the HRESIMS gave ions at *m/z* 485.1800 and *m/z* 507.1620, corresponding to [M + H]$^+$ and [M + Na]$^+$ for a molecular formula of C$_{26}$H$_{28}$O$_9$ (Figure S22, Supporting Information). The corresponding calculated values are 485.1812 and 507.1631. The NMR spectra showed the appropriate numbers of ^{1}H and ^{13}C signals (Table 2, Figures S23 and S24, Supporting Information). No significant fragmentation was seen in the MS.

Table 2. ^{1}H and ^{13}C NMR Spectroscopic Data for **4,5,7** in Methanol-d_4 [δ$_H$, multiplicity, (*J* (Hz))] [δ$_C$, Type]

position	4		5		7	
	δ$_H$	δ$_C$	δ$_H$	δ$_C$	δ$_H$	δ$_C$
1	2.34 m 1.36 ddd (13.0, 12.5, 4.0)	27.5, CH$_2$	1.23 m 2.10 m	25.2, CH$_2$	2.07 m 2.23 m	22.7, CH$_2$
2	2.00 m 1.71 ddd, (13.5, 13.0, 4.0)	30.5, CH$_2$	2.17 m 1.99 m	39.3, CH$_2$	1.24 m 1.45 m	32.9, CH$_2$
3	3.64 dd (12.5, 5.0)	77.2, CH	3.89 dd, (11.5, 6.0)	75.3, CH	3.85 dd, (11.5, 6.0)	73.4, CH
4	-	77.7, C$_q$	-	85.8, C$_q$	-	85.6, C$_q$
5	2.64 d (14.0)	55.4, CH	2.14 m	53.6, CH$_2$	-	49.8, C$_q$
6	-	213.9, C=O	-	107.7, C$_q$	-	108.6, C$_q$
7	2.78 dd (17.0, 12.5) 2.26 dd (17.0, 5.5)	46.2, CH$_2$	2.49 m	39.7, CH$_2$	2.24m 2.00 m	37.6, CH$_2$

8	2.08 m	37.8, CH$_2$	1.83 dd (12.5, 6.5)	37.4, CH	2.29 m	36.3, CH
9	-	52.5, C$_q$	-	51.6, C$_q$	-	50.1, C$_q$
10	2.34 m	46.0, CH	1.45 m	47.8, CH	1.44 m	43.7, CH
11	2.62 dd (14.0, 8.5) 2.50 dd (14.0, 8.5)	40.1, CH$_2$	2.14 m	33.7, CH$_2$	2.44 m 2.22 m	41.1, CH$_2$
12	5.57 t (8.5)	74.3, CH	5.46 m	73.9, CH	4.83 dd (8.5, 2.5)	68.4, CH
13	-	126.6, C$_q$	-	126.6, C$_q$	-	132.2, C$_q$
14	6.49 d (1.0)	109.3, CH	6.48 d (1.5)	109.2, CH	6.47 s	109.6, CH
15	7.62 br s	145.6, CH	7.54 brt (1.5)	145.7, CH	7.44 s	144.5, CH
16	7.54 t (1.5)	141.6, CH	7.61 brd (1.0)	141.7, CH	7.46 s	139.9, CH
17	1.00 d (7.0)	18.1, CH$_3$	1.02 d (7.0)	17.4, CH$_3$	0.85 d (7)	16.6, CH$_3$
18	4.82 d (12.5) 4.64 d (12.5)	65.5, CH$_2$	4.23 d (10.0) 3.99 d (10.0)	74.9, CH$_2$	4.38 d (10) 3.99 d (10)	75.6, CH$_2$
19	-	-	-	-	4.65 d (8.5) 4.60 d (8.5)	63.5, CH$_2$
20	-	179.1, C=O	-	178.9, C=O	-	174.8, C=O
1'	-	168.1, C=O	-	-	-	-
2'	-	122.1, C$_q$	-	-	-	-
3'	7.84 d (9.0)	132.9, CH	-	-	-	-
4'	6.83 d (9.0)	116.2, CH	-	-	-	-
5'	-	163.7, C$_q$	-	-	-	-
6'	6.83 d (9.0)	116.2, CH	-	-	-	-
7'	7.84 d (9.0)	132.9, CH	-	-	-	-

As before, the 1D and 2D NMR data of **4** (Table 2) strongly suggested a neoclerodane diterpenoid structure but with two striking differences from **1-3** (Figures S25-S28, Supporting Information). Firstly, the C-6 chemical shift at δ_C 213.9 indicated that the carbinol functionalities in **1-3** were replaced by a carbonyl group. Secondly, [1]NMR signals were seen at δ_H 6.83 (2 H, d) and 7.84 (2 H, d), indicating a *para*-disubstituted benzene. H-5 resonates as a doublet with $^3J = 14.0$ Hz, thus the core of the structure is again a *trans*-decalin. The C-9 *spiro*-lactone moiety was demonstrated as for **2**. The chemical shift of H-12 (δ_H 5.57) is consistent with H-5 of a γ-lactone moiety and there is an HMBC connection between this proton and the lactone carbonyl carbon at δ_C 179.1. The *spiro*-lactone was located at C-9 by HMBC connections from H-11 (δ_H 2.50 and 2.62) to C-10 (δ_C 46.0); the attachment to the furanyl unit was shown by HMBC connections

from H-11 to C-13 (δ_C 126.6) and from H-12 to C-13 (δ_C 126.6), C-14 (δ_C 109.3), and C-16 (δ_C 141.6). The NOESY spectrum in the δ_H 2.0–2.7 region is unclear, precluding assignment of the configuration at C-9, thus it is assigned by analogy with **1**. The NOESY interaction between H$_3$-17 and H-11 is consistent with an equatorial orientation for the methyl group. Moreover, H-7$_{ax}$ (α-face) (δ_H 2.78) shows a *trans*-diaxial relationship with H-8 (δ_H 2.08), with $^3J_{7ax\text{-}8ax}$ = 12.5 Hz, confirming that H-8 occupies the β-face.

In the southern zone of the structure of **4**, the carbonyl group is confirmed as C-6 since the H$_2$-7 signals (δ_H 2.26 and 2.78) are significantly deshielded compared to their counterparts in **1-3**. There were confirmatory HMBC connections from C-6 (δ_C 213.9) to H$_2$-7 (δ_H 2.26 and 2.78) and to H-10 (δ_H 2.34). H-3 (δ_H 3.64) is α-axially oriented, as shown by the coupling with H-2$_{ax}$ (β) ($^3J_{ax\text{-}ax}$ = 12.5 Hz) and H-2$_{eq}$ (α) ($^3J_{ax\text{-}eq}$ = 5.0 Hz), placing 3-OH equatorial on the β-face. The mutually coupled doublets at δ_H 6.83 (2 H) and 7.84 (2 H) revealed the presence of a 4-hydroxybenzoyl unit. This was linked as an ester to C-18 by HMBC connections from H$_2$-18 (δ_H 4.64 and 4.82) to the ester carbonyl (δ_C 168.1). A NOESY cross-peak between the signals of the H-18 resonance at δ_H 4.64 and H-10 (δ_H 2.34) confirms that the methyl 4-hydroxybenzoate unit is located axially on the β-face, also showing that ring A occupies a chair conformation. Thus we propose structure **4** for fatimanone.

Compound 5. The HRESIMS of **5** shows a major peak at *m/z* 387.1411, corresponding to [M + Na]$^+$ (calcd. 387.1420) for a molecular formula of $C_{19}H_{24}O_7$ (Figure S29, Supporting Information). Signals for 21 protons were observed in the ^{1}H NMR spectrum in methanol-d_4, showing that three hydroxy groups are present (Figure S30, Supporting Information). No significant fragmentation was evident in the MS.

The ^{13}C NMR spectroscopic data of **5** (Table 2) showed signals for 19 carbons (Figure S31, Supporting Information). HSQC and HMBC strongly suggested that this compound had the neoclerodane structure but lacked C-19 (Figures S32-S35, Supporting Information). Moreover, the ^{1}H and ^{13}C NMR spectra resembled those of **2** and **4**, showing the presence of the *spiro*-lactone at C-9, with the adjacent furanyl moiety. H-12 resonated at δ_H 5.46, consistent with furanCHO-carbonyl. This part of the structure was confirmed by HMBC cross-peaks between H-12 and C-9 (δ_C 51.6), C-13 (126.6), C-14 (109.2), and C-16 (141.7). H-3 (δ_H 3.89) resonates as a doublet of doublets, with $^3J_{ax-ax} = 11.5$ Hz and $^3J_{ax-eq} = 6.0$ Hz, which indicate that it is in an axial position. Since H-10 is β-axially oriented, HO-3 must occupy the β-face. A NOESY interaction between H-3 and H-5 (δ_H 2.14) showed that H-5 is also axial and α, thus ring A is in a chair conformation and thus the bicycle is a *trans*-decalin. H-8 (δ_H 1.83) resonates as a dd, with $^3J_{ax-ax} = 12.5$ Hz and $^3J_{ax-eq} = 6.5$ Hz, indicating that it is axial. Since H-8 is on the β-face, ring B must also be a chair. The hemiacetal bridge on the β-face between C-4 and C-6 was demonstrated as follows. The H-18 diastereotopic proton resonating at δ_H 3.99 correlates in HMBC with C-3 (δ_C 75.3) and C-6 (δ_C 107.7). The H-18 at δ_H 4.23 also correlates with C-6 as well as C-5 (δ_C 53.6). The interactions of H_2-18 with C-6 confirm the presence of the tetrahydrofuran moiety involving both C-4 and C-6.

The structure and configuration of **5** were established by single crystal X-ray crystallography (page 41, Supporting Information). Crystallization of **5** from MeOH gave <u>orthorhombic crystals, $P2_12_12_1$, $a = 6.4987(3)$</u> Å, $b = $ <u>6.9114(3)</u> Å, $c = $ <u>41.4349(19)</u> Å, $V = 1861.05$ (15)
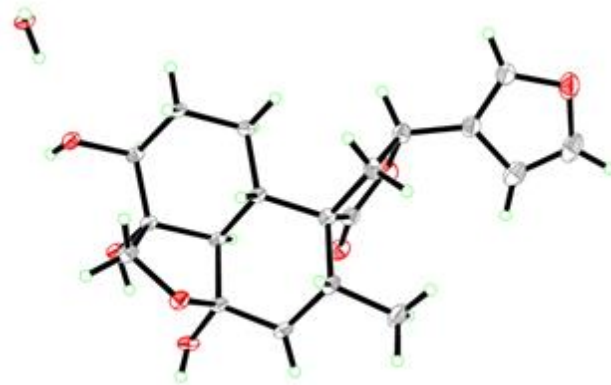

Figure 2. ORTEP diagram of a single molecule of **5**, with water of crystallization, from the X-ray crystal structure determination.

15

$Å^3$, $Z = 4$. The structure (Figure 2) contained one molecule of water of crystallization. This crystal structure confirmed the overall neoclerodane system, the *trans*-decalin configuration, the hemiacetal bridge and the (12S) and (8R) absolute configurations. The absolute configuration of compound **5** was established through the Flack parameter 0.00 (17). The structure of **5**, fatimanol D, is thus confirmed as shown.

Compound 6. For **6**, the HRESIMS shows a sodium adduct ion at *m/z* 459.1619, corresponding to a molecular formula of $C_{22}H_{28}O_9$ (calcd. [M + Na] = 459.1631) (Figure S36, Supporting Information). No peak was observed for $[M + H]^+$ but an ion at *m/z* 419 corresponds to loss of water from the protonated molecular ion and indicates the presence of a hydroxy group. Broad signals for three hydroxy group protons are present at δ_H 3.1, 4.5, and 4.7 in the ^1H NMR spectrum of **6** in $CDCl_3$ (Figure S37, Supporting Information).

Collectively, the NMR data of **6** (Table 3) (Figures S37-S42, Supporting Information) resembled those of **5**, but with H-5 substituted by an acetoxymethyl group. As usual, connectivity around the decalin was established by a combination of COSY, HSQC, and HMBC spectra (Figures S39-S42, Supporting Information). H-3 (δ_H 3.94) is axial, as shown by $^3J_{ax-ax} = 11.5$ Hz to the adjacent H-2$_{ax}$. H-3 also showed NOESY interactions with H-2$_{eq}$ (δ_H 1.50) and H-1$_{ax}$ (δ_H 2.23); the latter is only possible when H-1$_{ax}$ is cofacial with H-3$_{ax}$ and thus ring A is in a chair conformation. The -CH$_2$OAc group is shown by HMBC

Table 3. ^{1}H and ^{13}C NMR Spectroscopic Data for **6** in CDCl$_3$ [δ_H, Multiplicity, (J (Hz)] [δ_C, Type]

position	δ_H	δ_C
1	2.23 m	21.8, CH$_2$
	1.90 m	
2	1.23 m	32.1, CH$_2$
	1.50 m	
3	3.94 dd (11.5, 6.0)	72.5, CH
4	-	85.7, C$_q$
5	-	50.4, C$_q$
6	-	108.0, C$_q$
7	2.23 m	37.1, CH$_2$
	1.93 m	
8	1.88 m	36.9, CH
9	-	53.3, C$_q$
10	1.77 m	50.3, CH
11	2.47 m	42.3, CH$_2$
	2.34 m	
12	5.40 t (8.5)	71.8, CH$_2$
13	-	124.9, C$_q$
14	6.39 s	108.1, CH
15	7.44 s	144.4, CH
16	7.47 s	139.9, CH
17	1.05 d (7.0)	16.0, CH$_3$
18	4.40 d (10.0)	74.5, CH$_2$
	4.02 d (10.0)	
19	4.92 d (8.5)	62.1, CH$_2$
	4.83 d (8.5)	
20	-	176.8, C=O
1'	-	171.5, C=O
2'	2.07 s	21.4, CH$_3$

connections between H$_2$-19 (δ_H 4.83 and 4.92) and the ester carbonyl (δ_C 171.5). Further HMBC cross-peaks to the signals for C-4 (δ_C 85.7), C-6 (108.0), and C-10 (50.3) show that this acetoxy-methyl group is at C-5. A NOESY interaction between H$_2$-19 and H-1$_{ax}$ confirmed that the acetoxymethyl group is α-axially oriented, thus ring A occupies a chair conformation. This implies that H-10 is β-axially oriented, a conclusion that was confirmed by coupling with H-1. HMBC cross-peaks from H-18 at δ_H 4.40 to C-3 (δ_C 72.5) and C-6 (108.0) show that CH$_2$-18 is attached to C-4 with the hemiacetal functionality at C-6. This C-18 proton also shows a NOESY association with H-10 (δ_H 1.77), indicating that CH$_2$O-18 occupies the β-face and that C-18 and

the hemiacetal –O– at C-6 are both *pseudo*axial. Thus, ring B adopts a chair conformation and forms part of a *trans*-decalin core.

In the *spiro*-γ-lactone unit, H-12 resonates at δ_H 5.40 and H_2-11 at δ_H 2.34 and 2.47. HMBC cross-peaks between H-12 and C-14 (δ_C 108.1), C-13 (124.9), and C-16 (139.9) confirm that the furanyl moiety is joined to the lactone unit. HMBC cross-peaks between H-11 (δ_H 2.47) and C-8 (δ_C 36.9) and C-10 (50.3), between H-11 (δ_H 2.34) and C-10 (δ_C 50.3), and between H-10 (δ_H 1.77) and C-20 (δ_C 176.8) locate the *spiro*-lactone moiety at C-9. The configuration at this center is the same as in **1-5**, as indicated by a NOESY correlation between H-11 (δ_H 2.34) and H-10 (δ_H 1.77). NOESY correlations from H-12 (δ_H 5.40) to H-10 (δ_H 1.77) and H-1_{ax} (δ_H 2.23), are consistent with a (12*S*) absolute configuration. The signals for H-12 and H_3-17 (δ_H 1.05) are appropriately unconnected in NOESY. Interestingly, H_2-19 resonate at unusually low field (δ_H 4.83 and 4.92), due to their location in the deshielding plane of the anisotropic *spiro*-lactone carbonyl (vide supra). The (8*R*) absolute configuration is assigned by analogy with **1**-**5**. Thus we assign structure **6** for fatimanol E.

Compound 7. The HRESIMS of **7** shows a sodium adduct ion at *m/z* 417.1513 (calcd. 417.1525) for a molecular formula of $C_{20}H_{26}O_8$ (Figure S43, Supporting Information). The abundant ion at *m/z* 377 corresponds to loss of H_2O from the protonated molecular ion, indicating at least one hydroxy group. The ^1H NMR data (Table 2) contain signals for 26 protons and the ^{13}C spectrum contained 20 discrete peaks including a typical ester/lactone carbonyl (δ_C 174.8) (Figures S44, S45, Supporting Information). As for **1-6**, the HMBC connectivity showed the neoclerodane skeleton (Figures S46-S48, Supporting Information). H-3 is again shown by the values of the coupling constants to H-2_{ax} ($^3J_{ax-ax}$ 11.5 Hz) and H-2_{eq} ($^3J_{ax-ax}$ 6.0 Hz) to be β-

axially oriented. The acetal bridge between C-4 and C-6 is shown by HMBC connections between H_2-18 (δ_H 3.99 and 4.38) and C-3 (δ_C 73.4), C-4 (85.6), C-5 (49.8), and C-6 (108.6), the latter being particularly diagnostic of the closure of the cyclic hemiacetal moiety. A NOESY interaction between H-18 (δ_H 4.38) and H-10 (δ_H 1.44) places both C-18 and H-10 axial on the β-face and assigns the signal at δ_H 4.38 as H-18$_{endo}$.

Rather than forming a *spiro*-lactone, as in **2**, **4-6**, C-20 forms a bridging lactone with CH_2O-19, as shown by an HMBC connection between H_2-19 (δ_H 4.60 and 4.65) and C-3 (δ_C 73.4), C-4 (85.6), C-5 (49.8) and C-6 (108.6), the latter being particularly diagnostic of the closure of the hemiacetal ring. Since a NOESY interaction between H-10 and H-11 (δ_H 2.44) shows that CH_2-11 must be on the β-face, C-20 must be on the α-face. C-19 must also be on the α-face (Figure 3). Thus, **7** contains a *trans*-decalin moiety. The presence of the furan-CH(OH)-CH_2- unit at C-9 is confirmed *via* the HMBC cross-peaks of H_2-11 with C-10 (δ_C 43.7), C-12 (68.4), C-13 (132.2), and C-20 (174.8). H-12 (δ_H 4.83) resonates at a chemical shift appropriate for furanCHR(OH), rather than an ester function, and shows HMBC cross-peaks with C-9 (δ_C 50.1), C-13 (132.1), C-14 (109.6), and C-16 (139.9). It was not possible to determine the configuration at C-12.
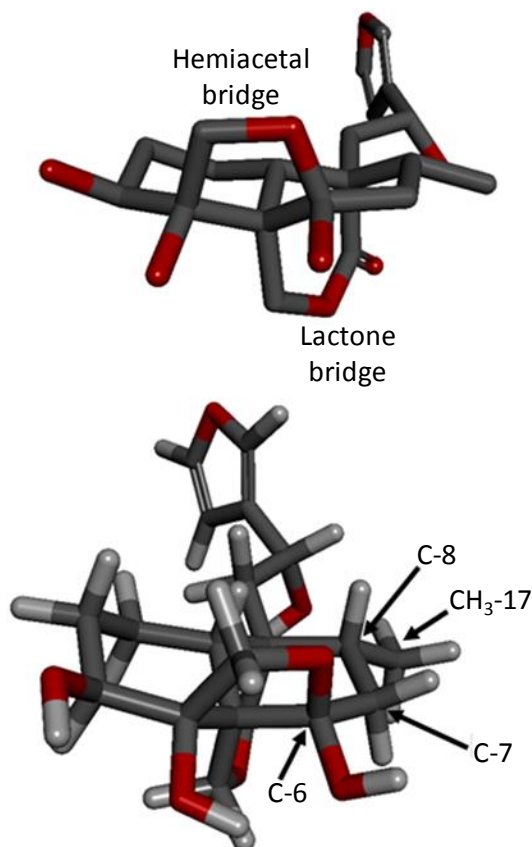

Figure 3. Upper: View (hydrogens omitted) of MM2-minimised structure of **7**, showing the hemiacetal and lactone bridges. **Lower:** Coplanarity of C-6, C-7, C-8 and CH_3-17 in MM2-minimised structure of **7**.

CH$_3$-17 (δ_H 0.85) is attached at C-8 (δ_C 36.3), as shown by HMBC cross-peaks to C-7 (δ_C 37.6),

C-8 (36.3), and C-9 (50.1), in addition to a weak interaction with C-6 (δ_C 108.6). Examination of

an MM2-minimized model of **7** suggests that CH$_3$-17, if equatorial and α, should make the (C-

17)-(C-8)-(C-7)-(C-6) unit antiperiplanar and consistent with a larger $^4J_{H\text{-}C}$ (Figure 3). Thus,

structure **7** is assigned to teulepicephin. This compound was isolated previously[14] from *Teucrium*

lepicephalum and *T. buxifolium* but only characterized as the 3-*O*-acetate acetyl derivative.

Li *et al*. have recently published a comprehensive review of clerodanes and related

compounds, including cataloguing their structures and biological activities.[23] The C-4 *spiro-*

oxirane moiety (in **1** and **3**) is present in a number of related natural products, including

clerodanes isolated from *Polyalthia longifolia* var. *pendula*[24] and *Teucrium polium*,[25] whereas

the 5-hydroxy furan-2(5*H*)-one feature (C-13, C-14, C-15, C-16) seen in **1** is less common, being

exemplified by salvidin B from *Salvia divinorum*[15] and rumphioside A from *Tinospora*

rumphii.[26] The lactol functionality in **2** is rare, having only been reported in teupestalin A[27] and

four compounds from *Teucrium* species.[6,28] Thus, the new compounds contain some features

which are unusual in naturally occurring clerodanes.

Biological evaluation

Compounds **1-7** were evaluated for
antimicrobial activity against the bacteria
Escherichia coli, Pseudomonas aeruginosa,
Staphylococcus aureus, Mycobacterium
smegmatis and the yeast *Candida albicans*.
No significant inhibitory activity was seen for

Table 4. Stimulation of the Growth of *E. coli* by **1** and **3**. Data Represent OD$_{600nm}$ of Wells as Percentages of No-drug Controls.

	Conc. (μM)	OD$_{600}$ as percentage of no-drug control
1	1037	234 ± 52
	519	273 ± 29
	259	226 ± 73
	130	154 ± 29
	65	130 ± 4
3	1073	200 ± 35
	536	238 ± 67
	268	273 ± 53
	134	122 ± 32
	67	129 ± 16

any compound against any of the five microorganisms (Figure S49, Supporting Information). However, **1** and **3** appeared to show concentration-related stimulation of the growth of *E. coli* at concentrations >100 μM (Table 4).

No cytotoxic activity was seen against HepG2 human hepatocellular carcinoma cells for **1-7** at concentrations <200 μM, using the MTT assay (Figure S50, Supporting Information).

Although extracts of plants in the *Teucrium* genus and the related *Lamiaceae* family have been widely reported to exhibit anthelmintic activities, the compound(s) responsible for these biological activities are still unclear.[9,29] Therefore, **1-7** were assessed for anthelmintic activities (phenotypes and motility) against the larval schistosomula lifecycle stage of *Schistosoma mansoni*. No activity was observed at 10 μM.[30] (Figures S51-S53, Supporting Information).

In this paper, we report the isolation and structural elucidation of six new neoclerodanes and a neoclerodane new to *T. yemense*. The new compounds combine structural features common in clerodanes with some of the more rare features. Cytotoxicity towards mammalian tumor cells has been reported for several clerodanes,[23] including the cesearupestrins.[31] Antifungal and antibacterial activities have also been reported for some examples but these clerodanes often have a narrow spectrum of activity.[23] However, **1-7** were shown to be devoid of such activity. Thus, the identification of the new neoclerodanes **1-6** contributes to the knowledge and understanding of the diversity of this important group of diterpenoids.

EXPERIMENTAL SECTION

General Experimental Procedures. The mp was measured on a Buchi Melting Point B-545 apparatus. The optical rotation was recorded on a Jasco Polarimeter P-2000 and UV was

recorded on a UV.1601 PC (Shimadzu) instrument. IR spectra were recorded on a Perkin-Elmer FTIR 600 series spectrometer. The 1D and 2D NMR spectra (^{1}H, COSY, NOESY, HSQC, and HMBC) were performed using Bruker spectrometers (500 MHz for ^{1}H and 175 MHz for ^{13}C NMR spectra). Conventional pulse sequences were used for COSY, HSQC, and HMBC. Chemical shift values are reported in δ (ppm), relative to internal TMS or residual solvent peak; coupling constants (*J*) are in Hertz (Hz). Ultra-high accuracy mass analysis was performed on a Nano-Flow (Triversa Nanomate; Advion Biosciences Limited, Norfolk, UK) linear trap quadrupole Fourier Transformation Ion Cyclotron Resonance Mass Spectrometry Ultra (FT-ICR-MS). Samples were reconstituted in HPLC-grade MeOH / ultra-pure water (7:3, 100 μL). Samples were vortexed and were centrifuged for 4 min at 13,000 rpm at 0 ºC. Supernatant (20 μL) was transferred to a clean well on a 128-well plate. Sample (13 μL) was injected by the nano-flow injection system, with an aliquot (5 μL) delivered to the ICR cell. Gas pressure was maintained at 0.5 psi with an applied voltage of 1.5 KV to maintain a consistent current of 60-120 nA. When operating in narrow SIM mode, the resolution was 100,000 and the scan window 30 *m/z*. Each scan was acquired in 60 sec. Column chromatography used normal-phase silica gel (Merck; 230-400 μm). HPLC was performed on a Shimadzu system (Kyoto, Japan), consisting of two LC-6AD Semi-Preparative Solvent Delivery pumps coupled with Rheodyne manual injector, communications bus module CBM-20A, a multi-wavelength photo-diode array detector (SPD-M20A), FRC-10A fraction collector, all connected to a computer system with Intel Core DUO with Microsoft XP and Shimadzu's LC solution software. It was fitted with two columns, Shim-pack PREP-ODS (H) Kit (A) 250 mm × 4.6 mm I.D., 5 μm particles (B) 250 mm × 20 mm I.D. Analytical HPLC was performed using the column under gradient conditions with mobile phase (MeCN / H$_2$O) programmed linearly to 100% MeCN during 35 min at 1.0 mL min^{-1}. The

UV detection wavelengths were 210 and 254 nm. The chromatographic separation HPLC was performed using column and preparative HPLC conditions as for analytical HPLC, except the flow rate was 20 mL min^{-1}.

Plant Material. *Teucrium yemense* (Defl.) was collected in February, 2014, from Aqabat Al-Abna, Baljurashi, Saudi Arabia, and was identified by taxonomist Dr. M. Yusuf, College of Pharmacy, King Saud University (KSU), Riyadh, Saudi Arabia. A voucher specimen (# 15292) has been deposited at the herbarium of the College of Pharmacy, KSU.

Extraction and Isolation. Dried and finely powdered aerial parts of *T. yemense* were defatted with *n*-hexane and extracted with MeOH. The EtOAc-soluble part of the MeOH extract was separated by column chromatography on silica gel to afford several fractions. Two polar fractions were subjected to repeated column chromatography and HPLC on an RP18 semi-preparative column, resulting in the isolation of **1**-**7** (Page 5, Supporting Information).

Fatimanol A (1): colorless gum; $[\alpha]^{21}_D$ +111 (0.055, MeOH); UV (MeOH) λ_{max}(log ε) 238 (3.37), 266 (3.22) nm; IR (KBr) ν_{max} 3412, 3004, 1730, 1716, 1420, 1362, cm^{-1}; ^{1}H and ^{13}C NMR, see Table 1; HMBC (Figure S6, Supporting Information), HRESIMS *m/z* [M + Na]$^+$ 505.2050, calcd. for $C_{24}H_{34}O_{10}Na$, 505.2040.

Fatimanol B (2): colorless gum; $[\alpha]^{21}_D$ -14.6 (0.015, MeOH); UV (MeOH) λ_{max}(log ε) 223 (1.20) nm; IR (KBr) ν_{max} 3602, 3404, 1714, 1423, 1363 cm^{-1}; for ^{1}H and ^{13}C NMR, see Table 1; HMBC (Figure S13, Supporting Information), HRESIMS *m/z* [M + Na]$^+$ 401.1567, calcd. for $C_{20}H_{26}O_7Na$, 401.1576.

Fatimanol C (3): colorless gum; $[\alpha]^{21}_D$ +26.4 (0.21, MeOH); UV (MeOH) λ_{max}(log ε) 226 (2.53) nm; IR (KBr) ν_{max} 3478, 2937, 1739, 1716, 1374, 1245 cm^{-1}; for ^{1}H and ^{13}C NMR, see Table 1; HMBC (Figure S20, Supporting Information), HRESIMS *m/z* [M + Na]$^+$ 489.2089, calcd. for $C_{24}H_{34}O_9Na$, 489.2101.

Fatimanone (4): colorless gum; $[\alpha]^{21}_D$ -25.7 (0.173, MeOH); UV (MeOH) λ_{max}(log ε) 222 (3.32), 269 (4.49), 329 (3.03) nm; IR (KBr) ν_{max} 3622, 2321, 1732, 1714, 1592, 1214 cm^{-1}; for ^{1}H and ^{13}C NMR, see Table 1; HMBC (Figure S27, Supporting Information), HRESIMS *m/z* [M + Na]$^+$ *m/z* 507.1620, calcd. for $C_{26}H_{28}O_9Na$, *m/z* 507.1631.

Fatimanol D (5): white crystals; mp 89-91 °C; $[\alpha]^{21}_D$ -34.2 (0.152, MeOH); UV (MeOH) λ_{max}(log ε) 232 (3.27) nm; IR (KBr) ν_{max} 3622, 3004, 1733, 1714, 1589, 1215 cm^{-1}; for ^{1}H and ^{13}C NMR, see Table 2; HMBC (Figure S34, Supporting Information), HRESIMS [M + Na]$^+$ *m/z* 387.1411, calcd. for $C_{19}H_{24}O_7Na$, *m/z* 387.1420.

Single crystals of **5** were obtained by slow evaporation from MeOH at room temperature. Data were collected on a Bruker APEX-II D8 Venture area diffractometer, equipped with graphite monochromatic CuK_α radiation, λ = 1.54178 Å at 100 (2) K. Cell refinement and data reduction were carried out by Bruker SAINT. SHELXT[32,33] was used to solve the structure. The final refinement was carried out by full-matrix least-squares techniques with anisotropic thermal data for non-hydrogen atoms on *F*. CCDC 1473246 contains the supplementary crystallographic data for this compound, which can be obtained free of charge from the Cambridge Crystallographic Data Centre *via* www.ccdc.cam.ac.uk/data_request/cif

Fatimanol E (6): colorless gum; $[\alpha]^{21}_D$ +15.2 (0.20, MeOH); UV (MeOH) λ_{max}(log ε) 231 (2.69) nm; IR (KBr) ν_{max} 3446, 2969, 1761, 1742, 1705, 1244 cm^{-1}; for ^{1}H and ^{13}C NMR, see Table 2; HMBC (Figure S41, Supporting Information), HRESIMS [M + Na]$^+$ *m/z* 459.1619, calcd. for $C_{22}H_{28}O_9Na$, *m/z* 459.1631.

Teulepicephin (7): colorless gum; $[\alpha]^{21}_D$ +3.4 (0.35, MeOH); UV (MeOH) λ_{max}(log ε) 232 (3.09) nm; IR (KBr) ν_{max} 3602, 3004, 1714, 1362,1222 cm^{-1}; for ^{1}H and ^{13}C NMR, see Table 2; HMBC (Figure S47, Supporting Information), HRESIMS [M + Na]$^+$ *m/z* 417.1513, calcd. for $C_{22}H_{30}O_{10}Na$, *m/z* 417.1525.

Compound Handling for Bioassays. Compounds **1-7** in DMSO (Fisher Scientific, Loughborough, UK) at concentrations of 10 mM and 1.6 mM were stored at -20°C.

Antimicrobial Assay. Bacterial suspensions were prepared by direct colony suspension. They were incubated overnight at 37°C in a temperature-controlled orbital shaker and were standardised to a McFarland standard value of 0.5 (1×10^8 cfu mL^{-1}) using a spectrophotometer.[34] Nutrient broth (190 μL) was added to each well in the 96-well plate. Further broth (160 μL) was added to wells A1-12, followed by test solution (40 μL). The sample was mixed, an aliquot (200 μL) was taken and added to each wells through to row E. Rifampicin (61 μM, control) was added to row F. The wells in rows G and H were left untreated. Standardised overnight culture (10 μL; 1×10^7 cfu mL^{-1}) was added to rows A-G to provide a final in-well concentration of 5×10^5 cfu mL^{-1}. Plates were incubated in a Hidex Sense Plate Reader (LabLogic, Sheffield UK) at 37°C and shaken at 300 rpm for 24 h. The optical density (OD) was measured at 600 nm every 20 min for 24 h.

MTT Cytotoxicity Assay. HepG2 cells (Sigma Aldrich, Gillingham, UK) were seeded at a density of 2.0×10^4 per well in a 96-well microtiter plate (Fisher Scientific, Loughborough, UK) in modified BME medium (50 μL; containing 1% antibiotic / mycotic (Sigma Aldrich, Gillingham, UK), 1% 200 mM L-Gln (Gibco, Paisley, UK), 1% MEM non-essential amino acid solution (Gibco, Paisley, UK) and 10% fetal bovine serum (Gibco, Paisley, UK). Cells were incubated in a humidified atmosphere containing 5% CO_2 at 37°C for 24 h prior to addition of compounds. Compounds were added to achieve final concentrations of 100-0.01 μM. After 20 h incubation, thiazolyl blue tetrazolium bromide [MTT; 5.0 μL, 12 mM (Sigma Aldrich, Gillingham, UK)] was added to each well. The culture medium was then removed gently after 4 h incubation. DMSO: isopropanol (1:1, 50 μL) was added and the plate was incubated for 15 min. The plate was agitated to ensure complete dissolution of formazan crystals and absorbance measurements (570 nm) were obtained at using a POLARstar Omega BMG Labtech v 1.02 plate reader. Blank wells, as well as positive (1% DMSO) and negative (1% Triton X-100, Fisher Bioreagents, Loughborough, UK) controls were incorporated in each plate.

Each data point represents a mean of three data sets (Supporting Information), with standard error presented. All absorbance readings were adjusted for background absorbance (eight blank wells per plate). Three positive (DMSO) and negative control (Triton X-100) wells were included, (1% final concentration) and gave absorbance readings of 0.578 (SE 0.031) and 0.024 (SE 0.004), respectively. All values have been adjusted for the background absorbance on the plate. The average (AVE) absorbance and standard deviation (SD) were calculated for each compound at each concentration.

Schistosoma mansoni **A**nthelmintic **S**creening. Potential anti-schistosomal effects of **1-7** (10 μM final concentration) were assessed on 24 h cultured schistosomula, according to the method described by Paveley.[30] Compounds **1-7** were prepared for screening in a 384-well plate (Perkin Elmer, MA, USA), where solutions (1.6 mM, 0.5 μL) were wet stamped using the Biomek NX[P] liquid handling platform into Basch medium (20 μL).[35] Controls were also wet stamped in the same manner, allowing for 16 wells each of DMSO (negative control) and Auranofin (Sigma, cat# A6733, positive control). Basch medium (60 μL), containing ~120 mechanically transformed schistosomula, were distributed into each treated well using a WellMate (Thermo Scientific, Loughborough, UK). The plate was incubated at 37°C for 24 h in a humidified atmosphere containing 5% CO_2. The plate was imaged using an ImageXpressXL high content imager (Molecular Device, UK) and further analyzed for effects on motility and phenotype, as previously reported by Paveley.[30]

ASSOCIATED CONTENT

*S Supporting Information

The Supporting Information (spectroscopic and crystallography data; data for antimicrobial, anthelmintic and cytotoxicity assays) is available free of charge on the ACS Publications website at DOI: ………………..

AUTHOR INFORMATION

Corresponding Authors

*Tel: +966114679196, Fax: +966114677245; E-mail: mohnalam@ksu.edu.sa (Mohammad Nur-e-Alam). Tel: +966114673741, Fax: +966114677245; E-mail: ajalreha@ksu.edu.sa (Adnan J. Al-Rehaily).

Author Contributions

The manuscript was written through contributions of all authors. All authors have given approval to the final version of the manuscript.

Notes

The authors declare no competing financial interests.

REFERENCES

(1) Moghtader, M.*, Am. Eurasian J. Agric. Environ. Sci.* **2009**, *5*, 843-846.

(2) Ulubelen, A.; Topcu, G.; Sonmez, U. Chemical and Biological Evaluation of Genus *Teucrium*, In *Studies in Natural Products Chemistry*; Atta-ur-Rahman, Ed.; 2000; Vol. 23, pp 591-648.

(3) Chaudhary, S. A. Flora of the Kingdom of Saudi Arabia Illustrated, Ministry of Agriculture and Water, National Agriculture and Water Research Center, Riyadh, Saudi Arabia. **2001**; Vol. 2, Part 2, 314.

(4) Bakhtiari, M.; Asgarpanah, J. *J. Essent. Oil Bearing Plants*, **2015**, *18*, 1174-1179.

(5) De la Torre, M. C.; Rodríguez, B.; Bruno, M.; Savona, G.; Piozzi, F**.;** Servettaz, O. *Phytochemistry* **1988**, *27*, 213-216.

(6) Carreiras, M.; Rodríguez, B.; Piozzi, F.; Savona, G.; Torres, M. R.; Perales, A. *Phytochemistry* **1989**, *28*, 1453-1461.

(7) González-Coloma, A.; Gutiérrez, C.; del Corral, J. M. M.; Gordaliza, M.; de la Puente, M. L.; San Feliciano, A. *J. Agric. Food Chem.* **2000**, *48*, 3677**-**3681.

(8) Jaradat, N. M. *Asian J. Pharm. Clin. Res.* **2015**, *8*, 13-19.

(9) Fatima, N. *Sci. Int. (Lahore)* **2016**, *28*, 1229-1231.

(10) Sattar, E. A.; Mossa, J. S.; Muhammad, I.; El-Feraly, F. S. *Phytochemistry* **1995**, *40*, 1737-1741.

(11) Sattar, E. A. *Arch. Pharm. Res*. **1998**, *21*, 785-786.

(12) Rahman, M. A.; Mossa, J. S.; Al-Said, M. S.; Al-Yahya, M. A. *Fitoterapia* **2004**, *75*, 149-161.

(13) Al-Musayeib, N. M.; Mothana, R. A.; Matheeussen, A.; Cos, P.; Maes, L. *BMC Comp. Alt. Med.* **2012**, 12, art. 49.

(14) Savona, G.; Piozzi, F.; Servettaz, O.; Rodríguez, B.; Hueso-Rodríguez, J. A.; de la Torre, M., *Phytochemistry* **1986**, *25*, 2569-2572.

(15) Shirota, O.; Nagamatsu, K.; Sekita, S. *J. Nat. Prod.* **2006**, *69*, 1782-1786.

(16) Coll, J.; Tandrón, Y. A. *Phytochem. Rev.* **2008**, *7*, 25-49.

(17) Lee, D. Y. W.; Ma, Z.; Liu-Chen, L-Y.; Wang, Y.; Chen, Y.; Carlezon., W. A.; Cohen, B. *Bioorg. Med. Chem.* **2005**, *13*, 5635-5639.

(18) Bedir, E.; Manyam, R.; Khan, I. A. *Phytochemistry* **2003**, *63*, 977-983.

(19) Coll, J.; Tandrón, Y. A. *Phytochemistry* **2005**, *66*, 2298-2303.

(20) Rollinson, D.; Knopp, S.; Levitz, S.; Stothard, J. R.; Tchuentée, L.-A. T.; Garba, A.; Mohammedi, K. A.; Schur, N.; Person, B.; Colley, D. G.; Utzinger, J. *Acta Tropica* **2013**, *128*, 423-440.

(21) Al-Yahya, M. A.; Muhammad, I.; Mirza, H. H.; El-Feraly, F. S.; McPhail, A. T. *J. Nat. Prod.* **1993**, *56*, 830-842.

(22) Pascual, C.; Fernández, P.; Garcia-Alvarez, M. C.; Marco, J. L.; Fernández-Gadea, F.; de la Torre, M. C.; Hueso-Rodríguez, J. A.; Rodríguez, B.; Bruno, M.; Paternostro, M.; Piozzi, F.; Savona, G. *Phytochemistry* **1986**, *25*, 715-718.

(23) Li, R.; Morris-Natschke, K. L.; Lee, K-H. *Nat. Prod. Rep.* **2016**, *33*, 1166-1226.

(24) Lee, T.-H.; Wang, M.-J.; Chen, P.-Y.; Wu, T.-Y.; Wen, W.-C.; Tsai, F.-Y.; Lee, C.-K. *J. Nat. Prod.* **2009**, *72*, 1960-1963.

(25) Alcázar, R.; de la Torre, M. C.; Rodríguez, B.; Bruno, M.; Piozzi, F.; Savona, G.; Arnold, N. A. *Phytochemistry* **1992**, *31*, 3957-3966.

(26) Martin, T. S.; Ohtani, K.; Kasai, R.; Yamasaki, K. *Phytochemistry* **1995**, *40*, 1729-1736.

(27) De la Torre, M. C.; Rodríguez, B.; Bruno, M.; Savona, G.; Piozzi, F.; Perales, A.; Torres, M. R.; Servettaz, O. *Phytochemistry* **1990**, *29*, 2229-2233.

(28) Bruno, M.; Omar, A. A.; Perales, A.; Piozzi, F.; Rodríguez, B.; Savona, G.; De la Torre, M. C. *Phytochemistry* **1991**, *30*, 275-282.

(29) Israili, Z. H.; Lyoussi, B. *Pak. J. Pharm. Sci.* **2009**, *22*, 425-462.

(30) Paveley, R. A.; Mansour, N. R.; Hallyburton, I.; Bleicher, L. S.; Benn, A. E.; Mikic, I.; Guidi, A.; Gilbert, I. H.; Hopkins, A. L.; Bickle, Q. D. *PLOS Neglect. Trop. D.* **2012**, *6*, e1762.

(31) Vieira-Júnior, G. M.; Dutra, L. A.; Ferreira, P. M. P.; de Moraes, M. O.; Costa Lotufo, L. V.; Pessoa, C. do Ó.; Buzanelli Torres, R.; Boralle, N.; Bolzani, V. da S.; Cavalheiro, A. J. *J. Nat. Prod.* **2011**, *74*, 776-781.

(32) Sheldrick, G. M. *Acta Cryst. A.* **2008**, *64*, 112–122.

(33) Sheldrick, G.M., SHELXTL-PC (Version 5.1), Siemens Analytical Instruments, Inc., Madison, WI, 1997.

(34) Wiegand, I.; Hilpert, K.; Hancock, R. E. *Nature Protoc*. **2008**, *3*, 163-175.

(35) Basch, P. F. *J. Parasitol.* **1981**, *67*, 186-190.

Graphical abstract